The Structural Basis for the Perturbed pK_a of the Catalytic Base in 4-Oxalocrotonate Tautomerase: Kinetic and Structural Effects of Mutations of Phe-50[†]

Robert M. Czerwinski,[‡,||] Thomas K. Harris,[§,||,⊥] Michael A. Massiah,[§,||] Albert S. Mildvan,*[,§] and Christian P. Whitman*[,‡]

Department of Biological Chemistry, The Johns Hopkins School of Medicine, 725 North Wolfe Street, Baltimore, Maryland 21205-2185, and Medicinal Chemistry Division, College of Pharmacy, The University of Texas, Austin, Texas 78712-1074

Received October 24, 2000

ABSTRACT: The amino-terminal proline of 4-oxalocrotonate tautomerase (4-OT) functions as the general base catalyst in the enzyme-catalyzed isomerization of β,γ-unsaturated enones to their α,β-isomers because of its unusually low pK_a of 6.4 ± 0.2, which is 3 units lower than that of the model compound, proline amide. Recent studies show that this abnormally low pK_a is not due to the electrostatic effects of nearby cationic residues (Arg-11, Arg-39, and Arg-61) [Czerwinski, R. M., Harris, T. K., Johnson, Jr., W. H., Legler, P. M., Stivers, J. T., Mildvan, A. S., and Whitman, C. P. (1999) *Biochemistry 38,* 12358−12366]. Hence, it may result solely from a low local dielectric constant of 14.7 ± 0.8 at the otherwise hydrophobic active site. Support for this mechanism comes from the study of mutants of the active site Phe-50, which is 5.8 Å from Pro-1 and is one of 12 apolar residues within 9 Å of Pro-1. Replacing Phe-50 with Tyr does not significantly alter k_{cat} or K_m and results in a pK_a of 6.0 ± 0.1 for Pro-1 as determined by ^{15}N NMR spectroscopy, comparable to that observed for wild type. ^{1}H-^{15}N HSQC and 3D ^{1}H-^{15}N NOESY HSQC spectra of the F50Y mutant demonstrate its conformation to be very similar to that of the wild-type enzyme. In the F50Y mutant, the pK_a of Tyr-50 is increased by two units from that of a model compound *N*-acetyltyrosine amide to 12.2 ± 0.3, as determined by UV and ^{1}H NMR titrations, yielding a local dielectric constant of 13.4 ± 1.7, in agreement with the value of 13.7 ± 0.3 determined from the decreased pK_a of Pro-1 in this mutant. In the F50A mutant, the pK_a of Pro-1 is 7.3 ± 0.1 by ^{15}N NMR titration, comparable to the pK_a of 7.6 ± 0.2 found in the pH vs k_{cat}/K_m rate profile, and is one unit greater than that of the wild-type enzyme, indicating an increase in the local dielectric constant to a value of 21.2 ± 2.6. A loss of structure of the β-hairpin from residues 50 to 57, which covers the active site, and is the site of the mutation, is indicated by the disappearance in the F50A mutant of four interstrand NOEs and one turn NOE found in wild-type 4-OT. ^{1}H-^{15}N HSQC spectra of the F50A mutant reveal widespread and large changes in the backbone ^{15}N and NH chemical shifts including those of Gly residues 48, 51, 53, and 54 causing their loss of dispersion at 23 °C and their disappearance at 43 °C due to rapid exchange with solvent. These observations confirm that the active site of the F50A mutant is more accessible to the external aqueous environment, causing an increase in the local dielectric constant and in the pK_a of Pro-1. In addition, the F50A mutation decreased k_{cat} 167-fold and increased K_m 11-fold from those of the wild-type enzyme, suggesting an important role for the hydrophobic environment in catalysis, beyond that of decreasing the pK_a of Pro-1. The F50I and F50V mutations destabilize the protein and decrease k_{cat} by factors of 58 and 1.6, and increase K_m by 3.3- and 3.8-fold, respectively.

The active site environment of an enzyme can significantly perturb the pK_a value of a residue from that typically observed for the exposed amino acid in a small peptide (*1*). A classic example of this phenomenon is found in the enzyme acetoacetate decarboxylase (AAD),[1] where a pK_a value of ~6.0 has been determined for the ϵ-amino group of the active-site lysine (Lys-115) (*2*). This pK_a value, which

[†] This research was supported by the National Institutes of Health Grant GM-41239 and the Robert A. Welch Foundation (F-1334) to C.P.W. and the National Institutes of Health Grant DK28616 to A.S.M. T.K.H. was supported by a National Institutes of Health Postdoctoral Fellowship GM17514.

* Address correspondence to either author. C.P.W.: Tel: 512-471-6198; Fax: 512-232-2606; E-mail: whitman@mail.utexas.edu. A.S.M.: Tel: 410-955-2038; Fax: 410-955-5759; E-mail: mildvan@welchlink.welch.jhu.edu.

[||] These authors contributed equally to this paper.

[§] The Johns Hopkins School of Medicine.

[‡] The University of Texas at Austin.

[⊥] Present address: Department of Biochemistry and Molecular Biology, University of Miami School of Medicine, Miami, FL 33136.

[1] Abbreviations: AAD, acetoacetate decarboxylase; CAPS, 3-[cyclohexylamino]-1-propanesulfonic acid; ESI-MS, electrospray ionization mass spectrometry; HPLC, high-pressure liquid chromatography; HSQC, heteronuclear single quantum coherence; IPTG, isopropyl-β-D-thiogalactoside; Kn, kanamycin; LB, Luria-Bertani medium; NMR, nuclear magnetic resonance; NOESY, nuclear Overhauser effect spectroscopy; 4-OT, 4-oxalocrotonate tautomerase; PCR, polymerase chain reaction; SDS−PAGE, sodium dodecyl sulfate−polyacrylamide gel electrophoresis; TSP, sodium 3-(trimethylsilyl)-propionate-2,2,3,3-d_4.

10.1021/bi0024714 CCC: $20.00
Published on Web 01/23/2001

Scheme 1

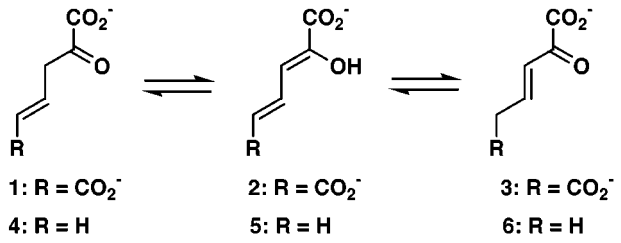

is 4.5 units lower than the pK_a of an exposed lysyl residue in solution, has been attributed to the proximity of the positively charged ϵ-ammonium group of Lys-116 (*2*). Recent site-directed mutagenesis studies of AAD confirmed the importance of the active site lysine in the mechanism as well as the effect of Lys-116 on the pK_a value of Lys-115 (*3*). Another example is provided by ketosteroid isomerase where the hydrophobic active site with a local dielectric constant of 18 ± 2 increases the pK_a values of Tyr-14 to 11.6 (*4*) and of Asp-99 to > 9 (*5*).

The active site environment in the bacterial isomerase, 4-oxalocrotonate tautomerase (4-OT, EC 5.3.2), also affects the pK_a value of a critical active site group (*6*−*12*). 4-OT catalyzes the isomerization of unconjugated α-keto acids such as 2-oxo-4-hexenedioate (**1**) to its conjugated isomer 2-oxo-3-hexenedioate (**3**) through the dienol intermediate 2-hydroxymuconate (**2**) (Scheme 1) (*6*). The enzyme catalyzes a suprafacial 1,3-allylic rearrangement using the amino-terminal proline as the general base catalyst (Figure 1) (*7*−*12*). Pro-1 can function as a general base under physiological conditions because of its unusually low pK_a of 6.4 (*10*), which is 3 units lower than the pK_a of the model compound, proline amide (*10*).

How the active site environment of 4-OT lowers the pK_a of Pro-1 has been the subject of much study (*8*, *10*, *13*, *14*). A crystal structure of 4-OT showed that several hydrophobic residues (Ile-2, Ile-5′, Ile-7′, Leu-8′, Ile-27, Leu-31, Ala-33, Pro-34, Val-38, Val-40, Met-45′, and Phe-50′)[2] surround Pro-1, within a sphere of 9 Å radius creating a site with a low dielectric constant (Figure 2) (*8*). In addition, two arginines, Arg-11′ and Arg-39″, which participate in catalysis are found at opposite sides of the active site cavity (Figures 1 and 2) (*13*). The hydrophobic environment coupled with the proximity of these two cationic residues was proposed to favor the neutral form of Pro-1, thereby lowering its pK_a (*8*, *10*). The effect of the two arginines on the pK_a of Pro-1 was recently investigated by replacing each arginine with an alanine (R11A and R39A) or a glutamine (R39Q) (*13*, *14*). In the R11A mutant, the pK_a of Pro-1 was comparable to that of the wild-type enzyme as demonstrated by direct ^{15}N NMR titration (pK_a = 6.3 ± 0.1) and by the pH dependence of k_{cat}/K_m (pK_a = 6.4 ± 0.2) (*14*). Replacing Arg-39 with an uncharged residue *lowered* the pK_a of Pro-1 below that observed for wild type. For the R39A mutant, the kinetically determined pK_a of Pro-1 was 5.0 (± 0.2), while for the R39Q mutant, it was 4.6 (± 0.2) (*14*). Also, since Arg-61 approaches the active site when Pro-1 is alkylated by an affinity label (*12*), the pK_a of Pro-1 in the R61A mutant was determined from the effect of pH on k_{cat}/K_m and found to be 6.5 ± 0.2 (*14*). On the basis of these observations, it was concluded that the electrostatic effects of nearby arginines do not contribute to the low pK_a of Pro-1.

In this study, the effect of the hydrophobic environment on the pK_a of Pro-1 was assessed by replacing Phe-50 with Tyr, Ala, Val, and Ile. Phe-50 is 5.8 Å from the amino terminal nitrogen of Pro-1 in the free enzyme (*12*) and is one of the 12 apolar residues composing the hydrophobic environment at the active site (Figure 2). The F50Y mutant was largely intact, both kinetically and structurally, permitting the use of Tyr-50 as a local probe of the dielectric constant near Pro-1. The F50V and F50I mutants were unstable, losing much of their initial catalytic activity over a 90-min period, precluding detailed kinetic and structural studies. However, the F50A mutant, although catalytically damaged, was stable enough to provide kinetic and structural evidence for increases in solvent accessibility, dielectric constant, and in the pK_a of Pro-1 at the active site. The present results, in combination with our previously reported study on the role of the active site arginines (*13*, *14*), implicate the low effective dielectric constant at the active site as the sole contributor to the unusually low pK_a of Pro-1. The results also demonstrate the key role played by Phe-50 in maintaining the structural integrity and hydrophobicity of the active site, thereby decreasing the pK_a of Pro-1 and promoting catalysis. A preliminary abstract of this work has been presented (*15*).

EXPERIMENTAL PROCEDURES

Materials. All reagents, buffers, and solvents were obtained from either Aldrich Chemical Co. or Sigma Chemical Co. unless noted otherwise. Tryptone and yeast extract were obtained from Difco (Detroit, MI). The YM-3 ultrafiltration membranes and Centricon (10 000 MW cutoff) centrifugal microconcentrators were obtained from Amicon. Isopropyl-β-D-thiogalactoside (IPTG) and thin-walled PCR tubes were obtained from Ambion, Inc. (Austin, TX). The syntheses of 2-hydroxymuconate (**2**, Scheme 1) and 2-hydroxy-2,4-pentadienoate (**5**, Scheme 1) are described elsewhere (*6*, *7*). The construction of the plasmid pETOT which contains the gene for 4-OT under control of the T7 expression system (pET system, Novagen, Inc., Madison WI) has been described (*9*). The expression vector pET24a was obtained from Novagen, Inc. Restriction enzymes, T4 DNA ligase, low melting point agarose, the Magic PCR Preps DNA purification kit, and the Wizard Plus Minipreps DNA Purification system were obtained from Promega Corp (Madison, WI). The Geneclean II kit was purchased from Bio 101, Inc (La Jolla, CA). The PCR was carried out using the PCR Reagent system from Promega Corp or the GeneAmp kit from Perkin-Elmer-Cetus (Norwalk, CT). Oligonucleotides for site-directed mutagenesis and DNA sequencing were synthesized by Oligos Etc. Inc (Wilsonville, OR).

Strains. *Escherichia coli* strain JM109 was obtained from Promega Corp and used for transformation of ligated plasmids. *E. coli* strain BL21(DE3)pLysS was obtained from Novagen and used for expression of the recombinant proteins. Cells for general cloning and expression were grown in LB media supplemented with kanamycin (50−100 μg/mL). The composition of LB medium is described elsewhere (*16*).

General Methods. Techniques for restriction enzyme digestions, ligation, transformation, and other standard mo-

[2] The unprimed, primed, and doubly primed residues come from different subunits of the 4-OT homohexamer.

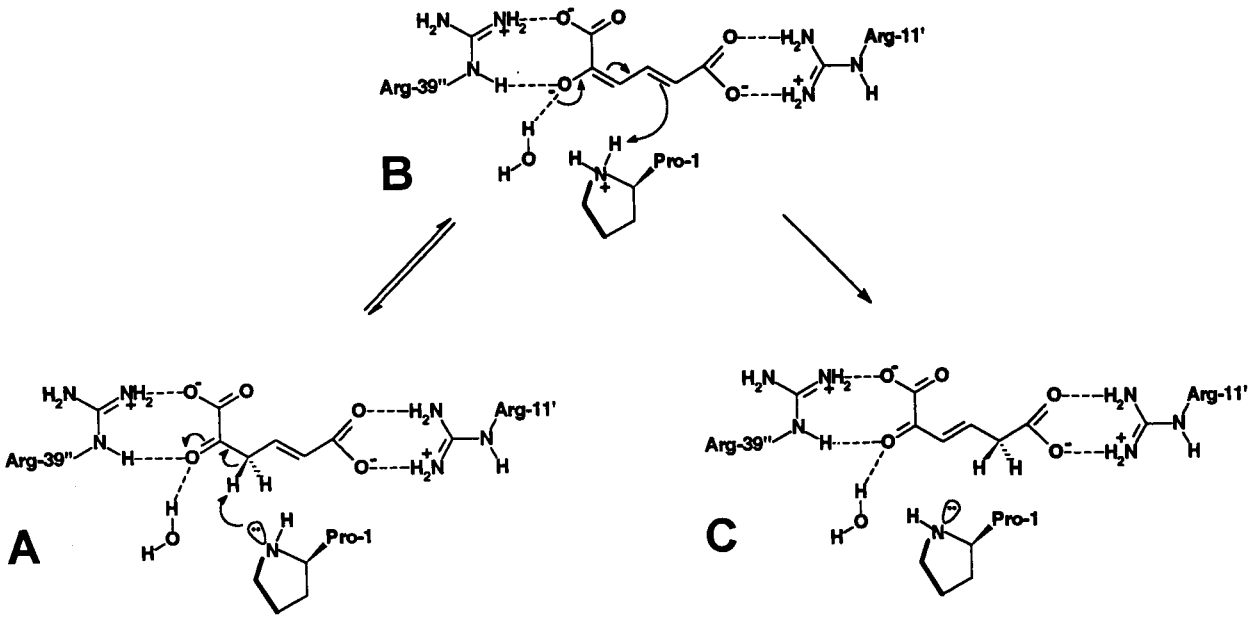

FIGURE 1: Mechanism of 4-OT consistent with crystallographic (*8*, *12*), NMR (*9*−*11*, *13*, *14*, *28*), and kinetic studies of the wild-type enzyme (*9*, *10*) and active site mutants (*11*, *13*, *14*).

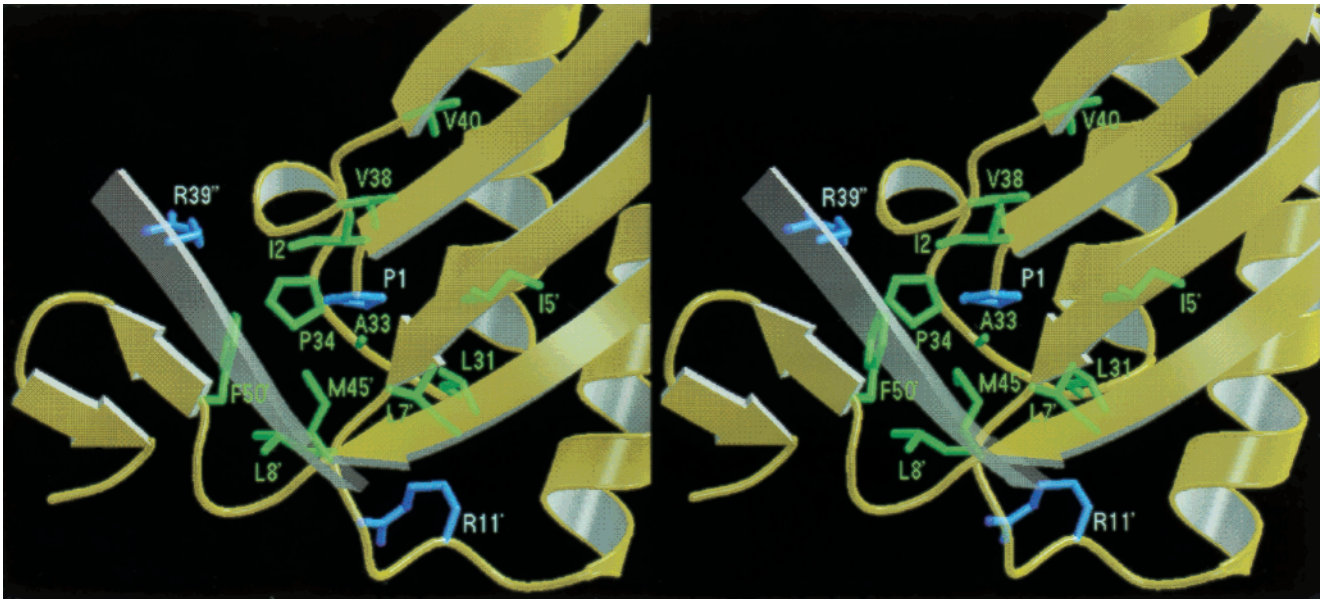

FIGURE 2: Stereopair of the active site of free 4-OT (*12*) showing hydrophobic residues within 9 Å of Pro-1 nitrogen. Hydrophobic residues are green and catalytic residues are blue. R11′ and R39″ come from different subunits than Pro-1. The β-hairpin is on the left. The gray β-strand bearing R39″ is closest to the reader.[2]

lecular biology manipulations were based on methods described elsewhere (*16*). DNA sequencing was done at the University of Texas (Austin) Sequencing Facility. Kinetic data and UV absorbance readings were obtained on a Hewlett-Packard 8452A Diode Array spectrophotometer. Enzyme activity was monitored by following the formation of **3** (Scheme 1) at 236 nm (*6*). The contents of the cuvettes were mixed by a stir/add cuvette mixer. The kinetic data were fitted by nonlinear regression data analysis using the Grafit program (Erithacus Software Ltd., Staines, U.K.) obtained from Sigma Chemical Co. HPLC was performed on a Waters system using either a Bio-Gel Phenyl 5-PW hydrophobic column or a Pharmacia Superose 12 (HR 10/30) gel filtration column. Protein was analyzed by tricine sodium dodecyl sulfate−polyacrylamide gel electrophoresis under denaturing conditions on 16% gels on a vertical gel electrophoresis apparatus obtained from Gibco (*17*). Trichloroacetic acid was used instead of acetic acid in the staining and destaining solutions. Protein concentrations were determined using the method of Waddell (*18*). Circular dichroic (CD) spectra were recorded at 25 °C in 20 mM sodium phosphate buffer (pH 7.3) at a concentration of approximately 10 μM (subunit concentration) on a Jasco J-600 spectropolarimeter equipped with an IBM Personal System II computer (model 55-SX) and on an AVIV 60DS spectropolarimeter with very similar results.

Site-Directed Mutagenesis. The four mutants of 4-OT (F50A, F50Y, F50V, and F50I) were prepared using the gene for 4-OT in the plasmid pETOT as the template (*9*). The gene is flanked by an *Nde*I restriction site and a *Sal*I restriction site. Mutations were made using the overlap extension polymerase chain reaction as described elsewhere

(*19*). The external PCR primers were oligonucleotides 5′-GATCTCGATCCCGCGAAATAAATACG-3′ (designated primer A) and 5′-CAGTGGTGGTGGTGGTGGTG-3′ (designated primer D). Primer A corresponds to the coding sequence of a region of the pET-24a(+) vector ~100 bp upstream from the *Nde*I restriction site while primer D corresponds to the complementary sequence of the His·Tag region of the pET-24a(+) vector, which is 24 bp downstream from the end of the coding sequence for 4-OT. For the F50A mutant, the internal PCR primers were oligonucleotides 5′-CCGATGCCGGCGTGGCCCTT-3′ (primer B) and 5′-AAGGGCCACGCCGGCATCGG-3′ (primer C). For the F50Y mutant, the internal PCR primers were oligonucleotides 5′-GCCGATGCCGTAGTGGCCCTT-3′ (primer B) and 5′-AAGGGCCACTACGGCATCGGC-3′ (primer C). For the F50V mutant, the internal PCR primers were oligonucleotides 5′-GCCGATGCCGACGTGGCCCTT-3′ (primer B) and 5′-AAGGGCCACGTCGGCATCGGC-3′ (primer C). For the F50I mutant, the internal PCR primers were oligonucleotides 5′-GCCGATGCCGATGTGGCCCTT-3′ (primer B) and 5′-AAGGGCCACATCGGCATCGGC-3′ (primer C). In each set of primers, primer C contains the codon for the desired mutation (underlined), while the remaining bases correspond to the coding sequence of the 4-OT gene. Primer B is the complementary primer with the desired codon underlined.

The PCR was carried out in a Perkin-Elmer DNA thermocycler 480 using template DNA, synthetic primers, and the PCR reagents following a protocol described elsewhere (*11*). The template DNA was prepared using the Wizard Plus Minipreps DNA Purification system as described (*11*). The AB and CD fragments were generated in separate PCRs as described (*11*). Subsequently, the mutated DNA fragment was produced by performing the PCR on a mixture of the AB and CD fragments (5 μL each) using primers A and D. The resulting gel-purified mutated DNA fragment and the pET24a(+) vector were digested with *Nde*I and *Sal*I restriction enzymes, purified, and ligated using T4 DNA ligase following a previously described protocol (*11*). Aliquots of the resulting mixture were transformed into competent *E. coli* JM109 cells and grown on LB/Kn (100 μg/mL) plates at 37 °C. Single colonies were chosen at random and grown in liquid LB/Kn media (50−100 μg/mL). The newly constructed plasmid was isolated and sequenced to verify the mutation. Subsequently, the mutated plasmid was transformed as described elsewhere into *E. coli* strain BL21(DE3)pLysS for protein expression (*11*).

Overexpression and Purification of Recombinant Enzymes. A single colony of the expression strain containing the desired plasmid was used to inoculate 25 mL of LB/Kn medium (50−100 μg/mL). After overnight growth at 37 °C, 3 mL of the culture was used to inoculate 500 mL of LB/Kn medium (50−100 μg/mL) in a 2 L Erlenmeyer flask. Cultures were grown to an OD_{600} of ~0.6 at 37 °C with vigorous shaking and then induced with IPTG (1 mM final concentration). Incubation was continued for 4 h at 37 °C. Cells were harvested by centrifugation (7000*g*, 12 min) and stored at −80 °C. Typically, 2 L of culture grown under these conditions yields 6 g of cells.

The mutants were purified to near homogeneity (>95% as assessed by SDS−PAGE) using a published procedure (*11*). Typically, the yields of purified enzyme per liter of culture ranged from 18 mg (F50V) to 75 mg (F50Y). The native molecular mass was estimated by size exclusion chromatography on a Superose 12 column. The mutant enzymes were chromatographed in 200 μL portions (~7 mg/mL) on the gel filtration column equilibrated with 20 mM sodium phosphate buffer, pH 7.3, at a flow rate of 0.2 mL/min. Protein was monitored at 254 nm. The mutants eluted at ~76 min.

Table 1: Kinetic Parameters for 4-OT and the F50 Mutants[a]

enzyme	k_{cat} (s^{-1})	K_m (μM)	k_{cat}/K_m (M^{-1} s^{-1})	relative (k_{cat}/K_m)
wild type	3500 ± 180	186 ± 25	1.9×10^7	1.0
F50Y	3200 ± 400	230 ± 60	1.4×10^7	0.7
F50A	21 ± 6	2000 ± 700	1.0×10^4	0.0005
F50I[b]	60 ± 6	610 ± 100	9.8×10^4	0.005
F50V[b]	220 ± 20	700 ± 90	3.1×10^5	0.016

[a] The steady-state kinetic parameters were determined in 50 mM sodium phosphate buffer, pH 7.5, at 23 °C. Errors are standard deviations. [b] The kinetic parameters were measured after 2 h when the activity had stabilized.

^{15}N Labeling of Wild Type, F50A, and F50Y 4-OT. The uniformly ^{15}N labeled enzymes were prepared in a MOPS-buffered medium by a protocol described elsewhere (*9*). The labeled enzymes were purified using a published procedure with the following modification (*11*). The active fractions eluting from the Bio-Gel Phenyl hydrophobic column were pooled, concentrated, and loaded on a Sephadex G-50 gel filtration column (60 × 3 cm) equilibrated with 20 mM sodium phosphate buffer (pH 7.3). At a flow rate of 0.5 mL/min, the protein eluted after 6 h and was collected in 10-mL fractions. The yields of purified enzymes per liter of culture medium were ~ 40 mg of ^{15}N-wild type 4-OT, ~7.5 mg of ^{15}N-F50A, and ~11 mg of ^{15}N-F50Y.

Mass Spectrometry. The monomeric masses of the purified mutant enzymes were determined by electrospray ionization mass spectrometry (ESI-MS) using a LCQ Finnigan octapole electrospray mass spectrometer. The samples for ESI-MS were prepared and analyzed as previously described (*13*). The observed monomeric molecular masses (MH^+) for the F50A, F50Y, F50V, and F50I mutants were 6735 (calc. 6734.7), 6828 (calc. 6826.8), 6763 (calc. 6762.8), and 6778 (calc. 6776.8) Da, respectively.

Kinetic Studies of the F50I and F50V Mutants. Two separate stock solutions (10 mL each), containing either 0.005 mg/mL of the F50I mutant or 0.002 mg/mL of the F50V mutant, were made up in 20 mM sodium phosphate buffer (pH 7.3). Aliquots (1 mL) were removed at different time intervals over a 90-min period and assayed for residual activity. The assay was initiated by the addition of **2** to give a final concentration of 250 μM. The kinetic parameters reported in Table 1 for the F50I and F50V mutants were measured after diluting the enzyme into 20 mM sodium phosphate buffer (pH 7.3) and allowing the solution to incubate for 2 h.

*pH Rate Profile of F50Y and F50A Using **2***. The pH dependences of the rates of ketonization of **2** to **3** by the F50Y and the F50A mutants of 4-OT were determined in 50 mM sodium phosphate buffer over the pH range 5.3−9.5 at 23 °C using the following modifications to a previously described procedure (*10*, *11*). For the F50Y mutant, the final enzyme concentrations were 530 nM (pH 4.7), 210 nM (pH 4.9), 100 nM (pH 5.2), 53 nM (pH 5.5−5.9), 21 nM (pH

6.1−6.3), 10 nM (pH 6.6−9.2), 16 nM (pH 9.4), 23 nM (pH 9.8−10.2), and 31 nM (pH 10.6−11.0). For the F50A mutant, the final enzyme concentrations were 22 μM (pH 5.3−6.1), 11 μM (pH 6.2−6.6), 5.4 μM (pH 6.8 and 9.5), and 3.3 μM (pH 7.0−9.1). It was necessary to use different enzyme concentrations of the mutants to facilitate the measurement of the reduced rates at the extreme pH values. The reaction was initiated by the addition of a quantity of **2** (final concentration 30−500 μM) from stock solutions made up in ethanol. The pH dependences of the kinetic parameters were fitted and analyzed as described previously (*10*, *11*).

*pH Rate Profile of F50Y Using 2-Hydroxy-2,4-pentadienoate (**5**).* The pH dependence of the rate of ketonization of 2-hydroxy-2,4-pentadienoate (**5**) to 2-oxo-3-pentenoate (**6**) by the F50Y mutant of 4-OT was determined in 50 mM sodium phosphate buffer over the pH range 5.0−11.0 at 23 °C using the following modifications to a previously described procedure (*10*, *11*, *14*). The final enzyme concentrations were 39 μM (pH 5.0−6.5) and 19 μM (pH 6.8−11.0). It was necessary to use different enzyme concentrations of the mutant at low pH to facilitate the measurement of the reduced rate. The rate of formation of **6** was monitored at 230 nm. The reaction was initiated by the addition of a quantity of **5** (final concentration 50−750 μM) from stock solutions made up in ethanol. The pH dependences of the kinetic parameters were fitted and analyzed as described previously (*10*, *11*, *14*).

pH Titration of Tyr-50 in the F50Y Mutant by Ultraviolet Spectroscopy. The UV spectrum of the F50Y (40 μM) mutant shows a λ_{max} at 278 nm in 50 mM Tris-HCl buffer (pH 7.5). In contrast, the wild-type enzyme has no λ_{max} at 278 nm because Phe-50, the only UV absorbing amino acid in 4-OT, does not absorb in this region. To determine the pK_a of Tyr-50, the changes in absorbance of the tyrosinate anion at 295 nm of the F50Y mutant were measured as a function of pH in the following 50 mM buffer solutions: Tris-HCl (pH 7.5−8.5); glycine (pH 8.7−9.5); CAPS (pH 9.7−10.8); and potassium phosphate (pH 11−13.2). The spectra were measured at 23 °C using 40 μM enzyme (in 1 mL samples) against a blank containing the same buffer. The pH was measured after the addition of the mutant enzyme to the buffer solution.

Structural NMR Methods. Unless otherwise stated, the solution conditions for the NMR studies of the uniformly ^{15}N-labeled F50Y and F50A mutants of 4-OT were 3.0 mM enzyme subunits, 8 mM sodium phosphate buffer, pH 6.4 ± 0.1, in 0.6 mL of 90% H_2O/10% D_2O. NMR data were collected at 43 °C for the F50Y mutant and at both 43 and 23 °C for the F50A mutant on a Varian UnityPlus 600 NMR spectrometer using a Varian 5-mm triple resonance probe with an actively shielded z-gradient. Multidimensional data sets were collected using the States-TPPI method (*20*) in the indirect dimensions, with a recycle time of 1.3 s. The observed ^{1}H chemical shifts were referenced to the H_2O signals, which were 4.61 and 4.79 ppm downfield from external TSP at 43 and 23 °C, respectively, and are reported with respect to TSP. The ^{15}N chemical shifts were measured with respect to external $^{15}NH_4Cl$ (2.9 mM in 1 M HCl) at 20 °C, which was 24.93 ppm downfield from liquid ammonia (*21*) and are reported with respect to liquid ammonia (*22*). Data were processed and analyzed on a Silicon Graphics Octane Workstation using the Felix 2.3 (Biosym Technologies, Inc.), NMRPipe (*23*), and NMRview (*24*) software packages.

^{1}H-^{15}N HSQC Spectra of the F50Y and F50A Mutants. ^{1}H-^{15}N HSQC spectra of the F50Y mutant were recorded at 43 °C, while the data for F50A mutant were recorded at both 43 and 23 °C using the fastHSQC pulse sequence (*25*). The spectral widths and acquired data points were 8000 Hz (^{1}H, *t2*, 1024 complex points) and 2000 Hz (^{15}N, *t1*, 128 complex points) using 8 transients per hypercomplex *t*1,*t*2 pair. For the ^{1}H and ^{15}N chemical shift comparisons between the wild-type, F50Y, and F50A mutant enzymes, ^{1}H-^{15}N HSQC spectra of wild-type 4-OT were collected at both 43 and 23 °C. The final processed data matrixes were 256 (*t*1) × 256 (*t*2) real data points.

3D ^{1}H-^{15}N NOESY HSQC Spectra of the F50Y and F50A Mutants. 3D ^{1}H-^{15}N NOESY HSQC spectra for the F50Y and F50A mutants were recorded with mixing times of 150 and 100 ms, respectively, using the pulse sequence previously described (*26*, *27*). The data were collected as follows: spectral widths, 8000 Hz (^{1}H, *t*3, 1024 complex points), 7200 Hz [^{1}H, *t*1, 256 (F50Y) or 150 (F50A) complex points], and 2000 Hz (^{15}N, *t*2, 64 complex points) with 8 and 16 transients for the F50Y and F50A mutants, respectively, per hypercomplex *t*1,*t*2 pair. The final processed data matrixes were 256 (*t*1,^{1}H) × 64 (*t*2,^{15}N) × 256 (*t*3, ^{1}HN) and 128 (*t*1,^{1}H) × 64 (t2,^{15}N) × 256 (*t*3, ^{1}HN) real data points for the F50Y and F50A mutants, respectively.

3D ^{1}H-^{15}N TOCSY HSQC Spectrum of the F50A Mutant. A 3D ^{1}H-^{15}N TOCSY HSQC spectrum was collected for the F50A mutant because it was determined from its ^{1}H-^{15}N HSQC spectrum that the chemical shifts of nearly all of the backbone ^{15}N and NH resonances had changed, requiring their reassignment. The data were collected and processed as described for the ^{1}H-^{15}N NOESY HSQC spectrum with the exception of collecting 128 complex points in the *t*2 dimension and using a TOCSY spin-lock time of 53 ms.

pH Titration of Pro-1 in the F50Y and F50A Mutants by ^{15}N NMR Spectroscopy and of Tyr-50 in the F50Y Mutant by ^{1}H NMR Spectroscopy. The pK_a values of Pro-1 in the F50Y and F50A mutants were determined by monitoring the pH dependence of its ^{15}N chemical shift. The ^{15}N NMR titrations were performed at 23 °C using 0.6-mL samples that were initially 3.0 mM (in subunits) of uniformly ^{15}N-labeled enzyme, containing 8 mM sodium phosphate buffer, pH 6.5, and H_2O/D_2O (90:10), by adding small amounts of 1 M HCl or 1 M NaOH. The ^{15}N NMR titrations of Pro-1 were found to be reversible in the pH range of 5.7−9.0, and each mutant enzyme retained ≥85% of its initial activity at the conclusion of the experiment. The ^{15}N NMR data were collected at 60.783 MHz without ^{1}H decoupling, using a Varian 5-mm broadband probe at 23 °C. The acquisition parameters were spectral width, 12 001 Hz; acquisition time, 0.683 s; relaxation delay, 1.0 s; total number of transients, 1400−7400.

The pK_a of Tyr-50 in the unlabeled F50Y mutant was determined at 23 °C by monitoring the pH dependence of chemical shifts of the aromatic side chain ^{1}Hδ- and ^{1}Hϵ-resonances of Tyr-50 using 0.6-mL samples that were initially 3.0 mM (in subunits) of unlabeled enzyme containing 50 mM sodium phosphate buffer, pH 7.5, and 99.99% D_2O. Small amounts of 1 M NaOD or DCl were added to the sample. The ^{1}H NMR spectra were acquired using the Varian

5-mm triple resonance probe with the following parameters: spectral width, 8000 Hz; acquisition time, 0.512 s; relaxation delay, 1.5 s; number of transients, 200.

The pK_a values for Pro-1 and Tyr-50 were determined from a nonlinear least-squares fit of the data to eq 1:

$$\delta(\text{ppm})^{\text{obs}} = \delta_1 + \delta_2(10^{\text{pH}-\text{p}Ka})^n/[(10^{\text{pH}-\text{p}Ka})^n + 1] \quad (1)$$

where n is the Hill coefficient, $\delta(\text{ppm})^{\text{obs}}$ is the observed chemical shift, and δ_1 and δ_2 are the limiting chemical shifts at low and high pH values, respectively.

RESULTS

Construction, Expression, and Characterization of the Mutants. The four mutants of 4-OT were constructed by overlap extension PCR, expressed in *E. coli* strain BL(DE3)-pLysS, and purified to homogeneity (as assessed by SDS−PAGE) using previously described procedures (*11*). The sequence of each mutant was confirmed by DNA sequencing. The range of overproduction (per liter of culture) varied from 18 mg (F50V) to 75 mg (F50Y).

The purified mutants were also analyzed by electrospray ionization mass spectrometry and gel filtration chromatography. Typically, the sample generates one major peak in the mass spectrometer that corresponds to the expected subunit molecular mass of each mutant. Hence, the amino-terminal proline is not blocked by the N-terminal methionine. It was further shown by size exclusion chromatography that the native molecular masses for the mutants are comparable to that of wild type, indicating that the mutants, like the wild-type enzyme (*12*), are homohexamers in solution.

Kinetic Properties of the Phe-50 Mutants. To examine the role of Phe-50 in catalysis by 4-OT, the effects of mutating this residue to alanine, valine, isoleucine, and tyrosine on the kinetic parameters of 4-OT were studied. The observed values for k_{cat}, K_m, and k_{cat}/K_m at 23 °C are summarized in Table 1. The most conservative of these mutations is the replacement of Phe-50 with Tyr, which results in an enzyme with kinetic parameters comparable to those of wild type. The most drastic of the four mutations is the change of Phe-50 to Ala, which results in a 167-fold decrease in k_{cat}, an 11-fold increase in K_m, and a 1900-fold decrease in k_{cat}/K_m (Table 1).

Both the F50V and the F50I mutants showed a biphasic time-dependent loss of activity. An initial rapid loss of activity in the first 10 min was followed by a much slower decrease in activity over the next 80 min (data not shown). After 90 min, the activities of the two mutants stabilized, with the F50I mutant retaining approximately 20% of its initial activity and the F50V mutant retaining approximately 50% of its initial activity. Neither the F50Y nor the F50A mutants exhibited this time-dependent behavior. The kinetic parameters for the F50I and the F50V mutants were measured after a 2 h-period, and intermediate effects on both k_{cat} and K_m were found, in comparison to those measured for the F50A and F50Y mutants (Table 1).

Structural Properties of the F50Y and F50A Mutants. The CD spectra of the F50Y and F50A mutants showed only small changes, indicating no major alterations in the secondary structures of these mutants (data not shown). The ^{1}H-^{15}N HSQC spectrum of the F50Y mutant at 43 °C showed small changes in chemical shifts of backbone ^{15}N and NH resonances around the site of the mutation in the β-hairpin that covers the active site (residues 49−52, 58), as well as in residues 2, 7, 8, and 40, near the active site, and in the long helix (residues 19 and 25) (Figure 3, panels A−C). The backbone amide ^{15}N and ^{1}H assignments for the F50Y mutant were confirmed by comparison of NOE cross-peaks to the backbone NH resonances, obtained by 3D ^{1}H-^{15}N NOESY HSQC spectra, to those of wild type 4-OT in which complete ^{1}H, ^{15}N, and ^{13}C chemical shift assignments have been made (*28*). ^{1}H-^{15}N NOESY HSQC spectra showed little change in NOE intensities for all residues, indicating the conformation of F50Y to be very similar to that of the wild-type enzyme.

The ^{1}H-^{15}N HSQC spectrum of the F50A mutant even at 23 °C showed widespread changes in chemical shifts of backbone ^{15}N and NH resonances throughout the protein (Figure 3, panels D−F), in some cases abolishing the degeneracy of the residues within the hexamer. These changes required the reassignment of backbone ^{15}N and NH resonances using the ^{1}H-^{15}N TOCSY HSQC and ^{1}H-^{15}N NOESY HSQC experiments, and the re-determination of the solution secondary structure of the F50A mutant (Figure 4). Noteworthy are the large changes in backbone ^{15}N and NH chemical shifts of Gly residues 48, 51, 53, and 54 of the β-hairpin (Figure 3, panels D−F) resulting in their loss of dispersion at 23 °C and their disappearance at 43 °C (not shown) due to rapid exchange with solvent, indicating a significant change in the structure and/or dynamics of the β-hairpin (see below).

As determined by strong backbone NH_i-NH_{i+1} and αH_i-NH_{i+1} NOEs, and αH chemical shift indices, at 23 °C, the α-helix from Asp-14 to Ala-33 and the β-strands from Val-38 to Ala-46 and from Pro-1 to Glu-9 found in the wild-type enzyme were intact in the F50A mutant (Figure 4). However, the β-hairpin from residues 50 to 57 was not detected, on the basis of the loss of four interstrand NOEs (from Ala-50 NH to Ala-57 NH, from Gly-51 αH to Ala-57 NH, from Ile-52 NH to Leu-56 αH, and from Ile-52 NH to Glu-55 NH) and the loss of a turn NOE (from Gly-54 NH to Glu-55 NH) (Figure 5), which were present in the wild-type enzyme (*28*). These results suggest increased mobility or complete disorder in the β-hairpin, which in the wild-type enzyme covers the active site (Figure 2).

pH Titration of Pro-1 in the F50Y and F50A Mutants by ^{15}N NMR Spectroscopy. Figure 6 shows the effect of pH on the ^{15}N chemical shifts of Pro-1 in the F50Y and F50A mutants. The limiting ^{15}N chemical shifts of Pro-1 at low pH (δ_1) and at high pH (δ_2) in both mutants agreed with those of the wild-type enzyme (Table 2). Fitting the titration data of the F50Y mutant to eq 1 yields an apparent pK_a of 6.0 ± 0.1, comparable to that of the wild-type enzyme but with a Hill coefficient of 0.69 ± 0.04 which is significantly lower than that of the wild-type enzyme (Table 2) indicating negative cooperativity in the deprotonation of Pro-1. Such negative cooperativity in the deprotonation of Pro-1, with a similar Hill coefficient, was also detected kinetically in the effect of pH on k_{cat}/K_m of substrate **5** with the F50Y mutant (see below). Because the Hill coefficient with F50Y is not equal to 1.0, the apparent pK_a represents the average pK_a at all interacting sites of the homohexamer. An alternate explanation for the low Hill coefficient is that the F50Y mutant forms an asymmetric homohexamer with intrinsically different pK_a values among the six active sites. This is

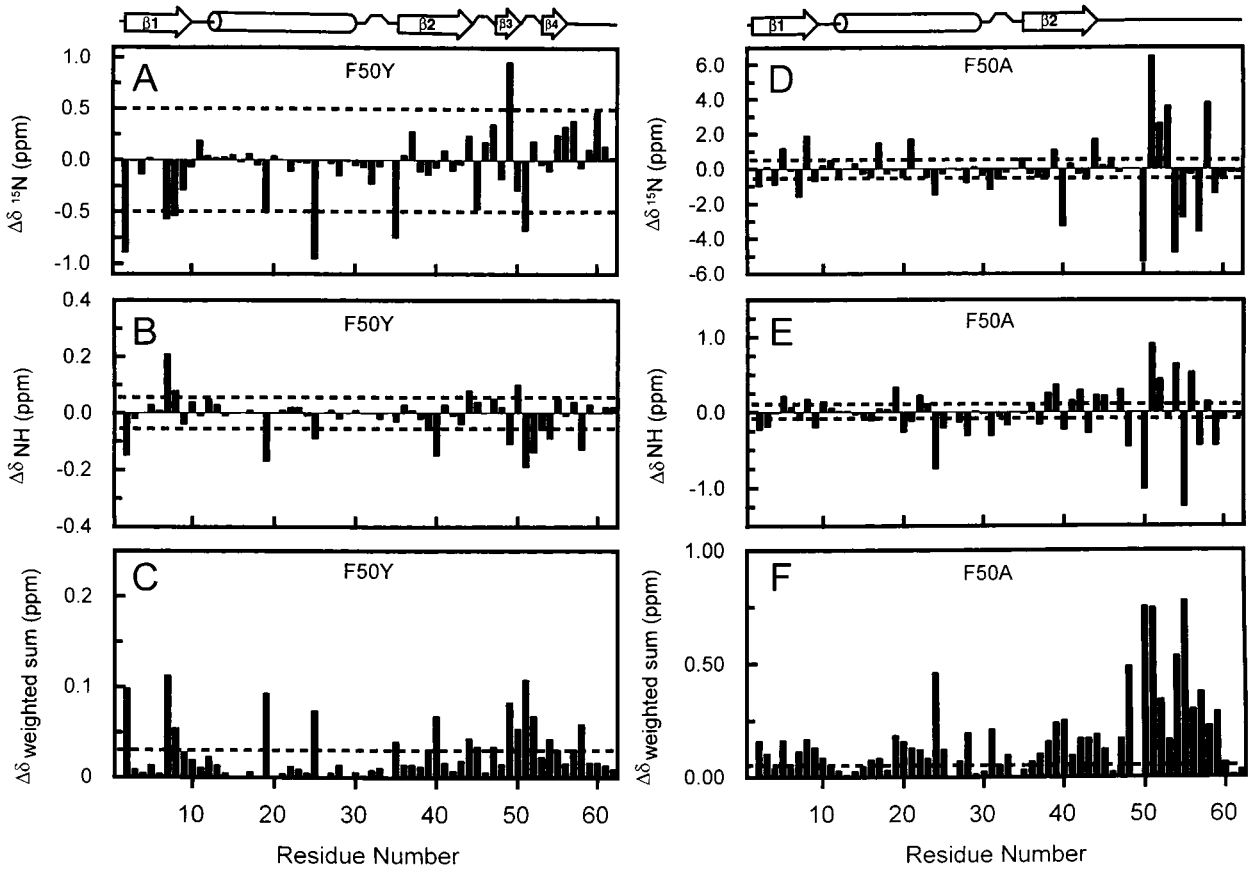

FIGURE 3: Backbone ^{15}N and NH chemical shift differences between wild type 4-OT and the F50Y (A−C) and the F50A mutant (D−F) enzymes. Chemical shift differences ($\Delta\delta = \delta_{\text{wild type}} - \delta_{\text{mutant}}$) were calculated from chemical shifts obtained by ^{1}H-^{15}N HSQC spectra at pH 6.4 ± 0.1, and at 43 °C (F50Y) or at 23 °C (F50A), and are plotted versus the residue number. Note the differences in chemical shift scales for the F50Y and F50A mutants. Control spectra of wild type 4-OT were obtained at both temperatures. (A, D) ^{15}N chemical shift differences. (B, E) ^{1}H chemical shift differences. (C, F) Sum of the absolute magnitudes of the ^{15}N and ^{1}H chemical shift changes, weighted according to the backbone amide chemical shift dispersions in the ^{15}N and ^{1}H dimensions (25.06 and 2.59 ppm, respectively, for the F50Y mutant; 25.55 and 1.87 ppm, respectively, for the F50A mutant. The dashed lines indicate the error limits. Also shown are the secondary structures of the two mutants.

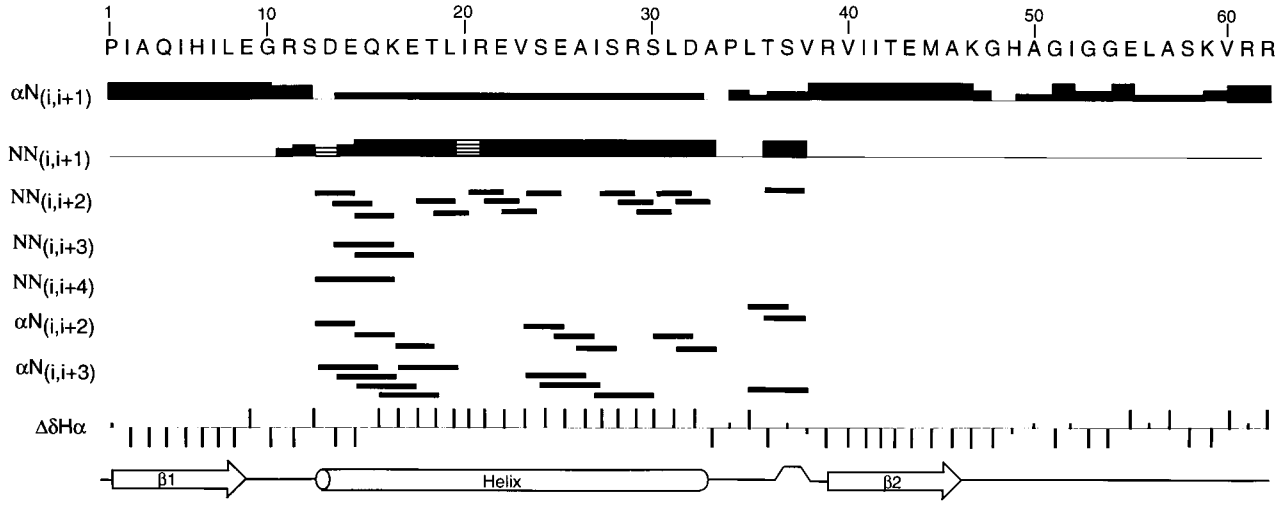

FIGURE 4: Diagram summarizing the sequential NOEs, the backbone Hα chemical shift indices, and the secondary structure of the F50A mutant of 4-OT at 23 °C. Crosshatched regions indicate ambiguous NOEs due to spectral overlap. The thicknesses of the bars represent the strengths of the NOEs. Short vertical lines indicate small, sub-threshold ΔδHα values.

unlikely because the ^{1}H-^{15}N HSQC spectrum of F50Y, like that of the wild type 4-OT, shows only 68 cross-peaks providing no evidence for asymmetry.

With the F50A mutant, the best fit of the ^{15}N NMR titration data of Figure 6 to eq 1 is obtained with a pK_a of 7.3 ± 0.1 significantly greater than that of the wild-type enzyme and a Hill coefficient of 1.0 ± 0.2 (Table 2). The loss of negative cooperativity in the deprotonation of Pro-1 may result from the disruption of the β-hairpin, which comes from a different subunit of the homohexamer.

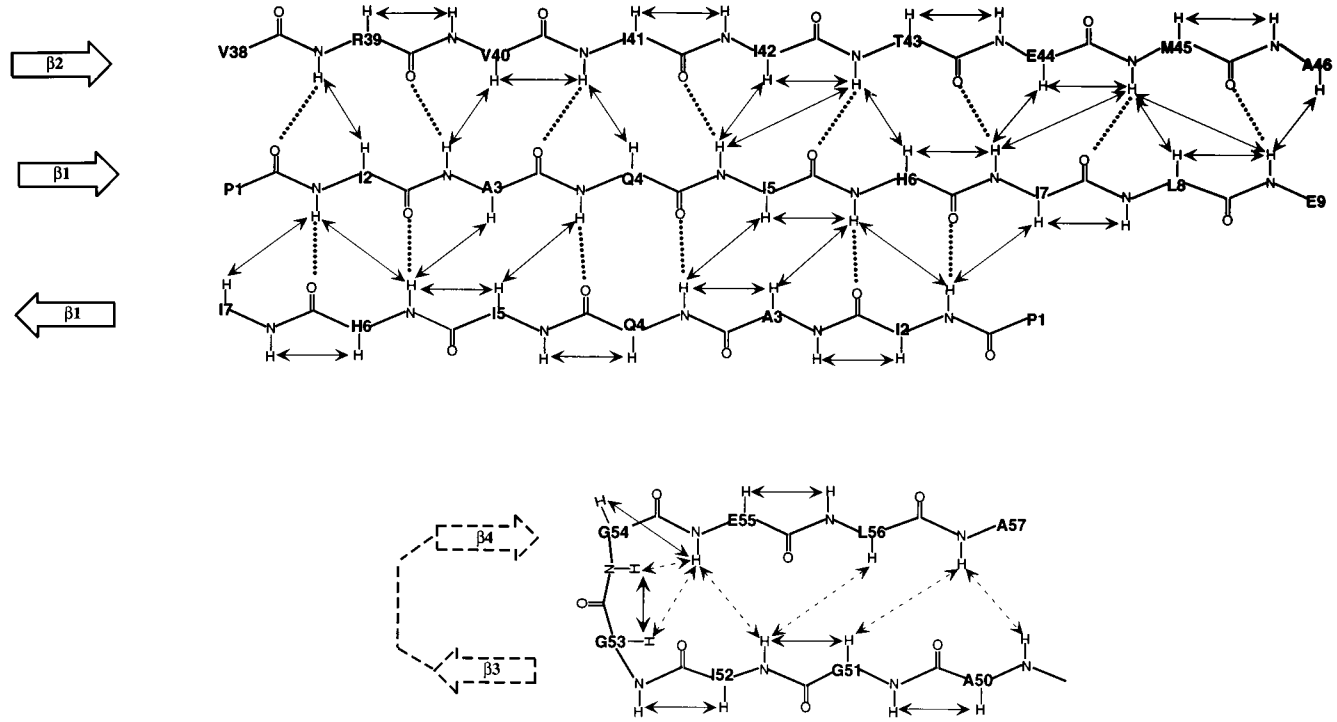

FIGURE 5: Diagram of the β-sheet structure of the F50A mutant of 4-OT. Solid double-headed arrows indicate sequential and cross-strand NOEs seen in ^{1}H-^{15}N 3D NOESY−HSQC spectra. Dotted lines indicate hydrogen bonds suggested by nearby NOE's. Dashed double-headed arrows indicate NOEs seen in the β-hairpin of wild type 4-OT but not found in the F50A mutant. The $\beta1-\beta1$ interaction is across a dimer interface, while the $\beta1-\beta2$ and $\beta3-\beta4$ interactions are intrasubunit, as found in wild type 4-OT (*28*).

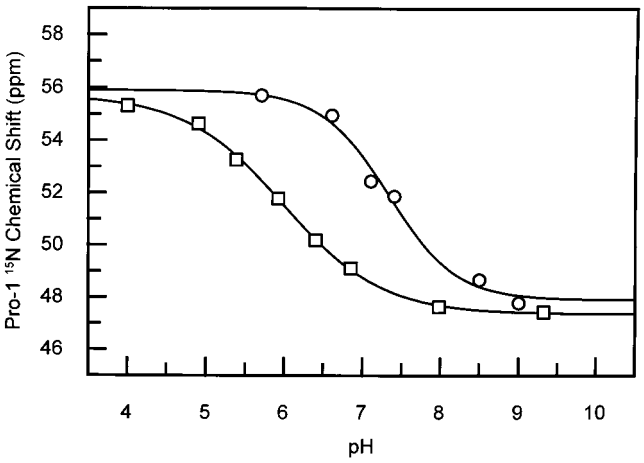

FIGURE 6: pH titration of the amino group of Pro-1 in the F50Y and F50A mutants of 4-OT monitored by ^{15}N NMR spectroscopy at 23 °C. The effect of pH on the ^{15}N chemical shift of Pro-1 in the F50Y mutant (squares) is fit by eq 1 using a Hill coefficient (n) of 0.69 ± 0.04 and a pK_a of 6.0 ± 0.1, and in the F50A mutant (circles) using a Hill coefficient of 1.0 ± 0.2 and a pK_a of 7.3 ± 0.1 (Table 3).

Table 2: ^{15}N NMR Titration Parameters of Proline-1 at 23 °C

enzyme	pK_a	n	δ_1 (ppm)	δ_2 (ppm)
WT[a]	6.4 ± 0.2	1.0 ± 0.05	55.6 ± 0.3	47.5 ± 0.2
F50Y	6.0 ± 0.1	0.69 ± 0.04	55.7 ± 0.2	47.4 ± 0.1
F50A	7.3 ± 0.1	1.0 ± 0.2	55.9 ± 0.4	47.9 ± 0.4

[a] T = 30 °C from ref *10*.

pH Dependence of the Kinetic Parameters of the F50Y Mutant. The large values of k_{cat} and k_{cat}/K_m for the F50Y-catalyzed ketonization of **2**, comparable to those of the wild-type enzyme, complicate a straightforward analysis of their pH dependences because **2** is a sticky substrate (*10*, *14*). Because the relative stickiness of the substrate and of protons to the enzyme are unknown, we have modeled the data using equilibrium assumptions as has been done previously for the wild-type enzyme (*10*) and the highly active R61A mutant (*14*). This analysis takes into account the pK_a of the 6-carboxylate group of the substrate (5.4 ± 0.1). For the reaction of the F50Y mutant using **2**, a plot of log(k_{cat}/K_m) vs pH was fit with the logarithmic form of eq 2 generating a bell-shaped curve with limiting slopes of 2 and 1 on the ascending and descending limbs, respectively (Figure 7, panel A).

$$k_{cat}/K_m = (k_{cat}/K_m)^{max}/ [(1 + [H^+]/K_a^{SH})(1 + [H^+]/K_{H2E} + K_{HE}/[H^+])] \quad (2)$$

In eq 2, K_a^{SH} is the ionization constant of the 6-carboxylic acid group of the free substrate **2**, and K_{H2E} and K_{HE} are the ionization constants for the base and acid catalysts, respectively, in the free enzyme. From this analysis, the apparent pK_a of Pro-1 is 5.3 ± 0.2 (Table 3), which agrees with that found for the wild-type enzyme using the sticky dicarboxylic acid substrate, **2** (pK_a = 5.2 ± 0.1). While the pK_a of the required protonated group (9.3 ± 0.5) appears to differ from that of the wild-type enzyme (10.3 ± 0.2) (*10*), the uncertainty in the former value is high (Table 3).

The effect of pH on the k_{cat} of the F50Y mutant using the sticky substrate **2** shows an ascending limb of unit slope followed by a plateau (Figure 7, panel A), yielding an apparent pK_a of 6.2 ± 0.1 for Pro-1 in the enzyme−substrate complex according to eq 3.

$$k_{cat} = (k_{cat})^{max}/(1 + [H^+]/K_{H2E}) \quad (3)$$

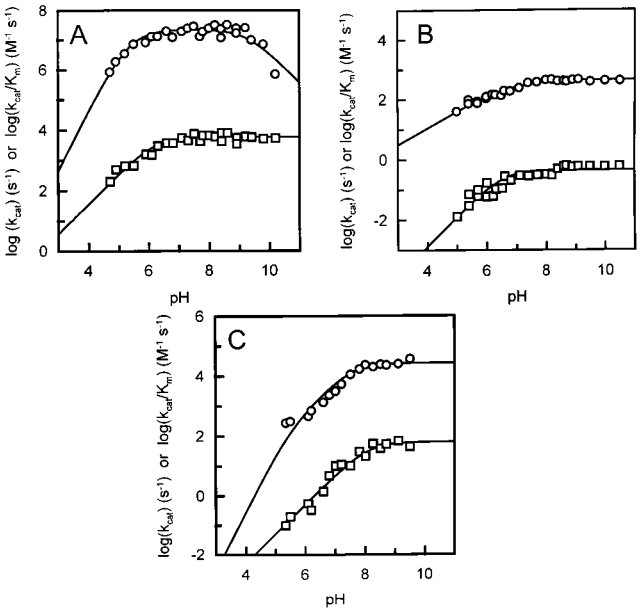

FIGURE 7: pH dependences of the kinetic parameters of the F50Y and F50A mutants of 4-OT. The effect of pH on log(k_{cat}/K_m) (circles) and log(k_{cat}) (squares) are shown for (A) the F50Y mutant enzyme using substrate **2**, (B) the F50Y mutant using substrate **5**, and (C) the F50A mutant using substrate **2**. The curves were computed from nonlinear least-squares fits of the data to eqs 2−4 as described in the text yielding the pK_a values given in Table 3.

This apparent pK_a overlaps with that found for the wild-type enzyme using **2** (Table 3) (*10*). The absence of a descending limb indicates that the pK_a of any required protonated group exceeds 10 in the enzyme−substrate complex with substrate **2**.

For the reaction of the F50Y mutant with the nonsticky substrate **5**, a plot of log(k_{cat}/K_m) vs pH shows an ascending limb with a slope less than 1 followed by a plateau (Figure 7, panel B). Assuming rapid equilibrium, the data can be fit to the logarithmic form of eq 4:

$$k_{cat}/K_m = (k_{cat}/K_m)^{max}/[1 + ([H^+]/K_{H2E})^n] \qquad (4)$$

where n is the Hill coefficient. The fit yields an apparent pK_a of 6.8 ± 0.1 and a Hill coefficient of 0.58 ± 0.10. While the Hill coefficient overlaps with that found by direct ^{15}N NMR titration, the apparent pK_a does not. The apparent pK_a of 6.8 determined kinetically represents the average pK_a at all interacting sites which are kinetically operative, while the pK_a of 6.0 ± 0.1 determined by ^{15}N NMR is the average of Pro-1 at all six sites of the homohexamer.

With the nonsticky substrate **5**, the effect of pH on k_{cat} of the F50Y mutant shows an ascending limb of unit slope followed by a plateau (Figure 7, panel B) yielding, from eq 3, a pK_a value for Pro-1 in the enzyme−substrate complex of 7.3 ± 0.3. This value overlaps with that found for the wild-type enzyme with the same substrate **5** (Table 3). The absence of a descending limb in the pH rate profiles for both k_{cat}/K_m and k_{cat} indicates that the pK_a of any required protonated group in both free F50Y and in its complex with substrate **5** exceeds 10.

pH Dependence of the Kinetic Parameters for the F50A Mutant. The decreased values of k_{cat} and k_{cat}/K_m for the F50A-catalyzed ketonization of **2** (Table 1) suggest that the enzyme−substrate complex is in rapid equilibrium with the free enzyme and substrate. Hence, the pH dependence of the steady-state parameters for **2** can be analyzed using rapid equilibrium assumptions as previously described (*10, 14*). For the F50A mutant, a plot of log k_{cat}/K_m vs pH for **2** shows an ascending limb followed by a plateau (Figure 7, panel C). A nonlinear least-squares fit of the pH dependence of k_{cat}/K_m to the logarithmic form of eq 2 which includes a constant for the ionization of **2**, and with $K_{HE} = 0$, gave a pK_a value for Pro-1 in the free enzyme of 7.6 ± 0.2 (Table 3). The agreement of this pK_a with that found by direct ^{15}N NMR titration of Pro-1 (7.3 ± 0.1, Tables 2 and 3) indicates that substrate **2** has become nonsticky in the F50A mutant as might be expected from its 167-fold lower k_{cat} and 11-fold greater K_m values in comparison with those of the wild-type enzyme (Table 1). The pK_a values for Pro-1 in the free F50A mutant, from both NMR titration (Table 2) and from k_{cat}/K_m vs pH, are ∼1.0 unit greater than those found in the wild-type enzyme (Table 3).

The plot of k_{cat} vs pH for **2** shows a single ascending limb with a slope of 1.0 (Figure 7, panel C). A nonlinear least-squares fit of the pH dependence of k_{cat} to the logarithmic form of eq 4 gave a pK_a value for Pro-1 in the enzyme−substrate complex of 8.1 ± 0.1, which is significantly greater than those found with the wild-type enzyme with both substrates **2** and **5** (Table 3). Also, unlike the wild-type enzyme, the F50A mutant showed no descending limbs in its pH rate profiles indicating a pK_a value >9.5 for any required protonated group.

Measurement of the pK_a Value of Tyrosine in the F50Y Mutant. The F50Y mutant, which has enzymatic activity comparable to the wild-type enzyme and has no other aromatic residues, is an ideal system in which to measure the pK_a of the tyrosine, and thereby to independently estimate the local dielectric constant near this residue. Accordingly, the pK_a of the phenolic hydroxyl group was measured by both ultraviolet absorption and ^{1}H NMR spectroscopy (Figure 8). The UV spectrum of the F50Y mutant at pH 7.5 showed an absorbance maximum at 278 nm. Increasing the pH from 10.5 to 13.4 causes an increase in the absorbance at 295 nm resulting in a peak due to the formation of the tyrosinate anion (*4*). However, nonisosbestic behavior was noted between 274 and 287 nm as the tyrosinate band at 295 nm increased between pH 11 and 12.9. This nonisosbestic behavior indicates other structural changes in the F50Y mutant at high pH values. The increases in absorbance at 295 nm as a function of pH were fit with an equation of the form of eq 1, in which δ_1 and δ_2 represent the limiting absorbances at low and high pH values, respectively. This fitting, using titration data from pH 8.5 to 13.4, yielded a pK_a of 12.0 ± 0.1 with a Hill coefficient of 1.2 ± 0.1 (Figure 8, panel A). The Hill coefficient slightly exceeding unity, like the nonisosbestic behavior, may reflect structural changes at high pH in addition to the ionization of tyrosine.

The pK_a of the phenolic hydroxyl group was independently measured by monitoring the changes in chemical shifts of the aromatic side chain δ- and ϵ-protons of Tyr-50 as a function of pH (Figure 8, panel B). The chemical shifts of these protons were typical for tyrosine residues of proteins (*29*). A nonlinear least-squares fit of the data to eq 1 gave a pK_a = 12.5 ± 0.1 with a Hill coefficient of 0.84 ± 0.10 for the ϵ-protons and a pK_a = 12.0 ± 0.1 with a Hill coefficient of 1.1 ± 0.2 for the δ-protons. The chemical shifts of the

Table 3: Summary of the pH Dependences of Kinetic Parameters and pK_a Values Determined by Direct ^{15}N NMR Titration for 4-OT and F50 Mutants at 23 °C

					pK_a[b]			
enzyme	substrate	$(k_{cat})^{max}$ (s^{-1})	$(k_{cat}/K_m)^{max}$ (M^{-1} s^{-1})	pK_a of Pro-1[a]	pK_{H2E}	pK_{HE}	pK_{H2ES}	pK_{HES}
wild type	**2**	3500 ± 500	1.9×10^7	6.4 ± 0.2[c]	5.2 ± 0.1[c]	10.3 ± 0.2[c]	6.5 ± 0.2[c]	9.6 ± 0.3[c]
	5	0.4 ± 0.02	3.6×10^2		6.2 ± 0.3	9.0 ± 0.3	7.7 ± 0.2	8.5 ± 0.3
F50Y	**2**	5900 ± 400	2.2×10^7	6.0 ± 0.1[d]	5.3 ± 0.2	9.3 ± 0.5	6.2 ± 0.1	*f*
	5	0.6 ± 0.03	4.6×10^2		6.8 ± 0.1[e]	*f*	7.3 ± 0.3	*f*
F50A	**2**	62 ± 2	2.6×10^4	7.3 ± 0.1	7.6 ± 0.2	*f*	8.1 ± 0.1	*f*

[a] From 1D ^{15}N NMR pH titration of Pro-1. [b] From the pH-rate profiles. [c] $T = 30$ °C. [d] Hill coefficient = 0.69 ± 0.04. [e] Hill coefficient = 0.58 ± 0.10. [f] No descending limb detected.

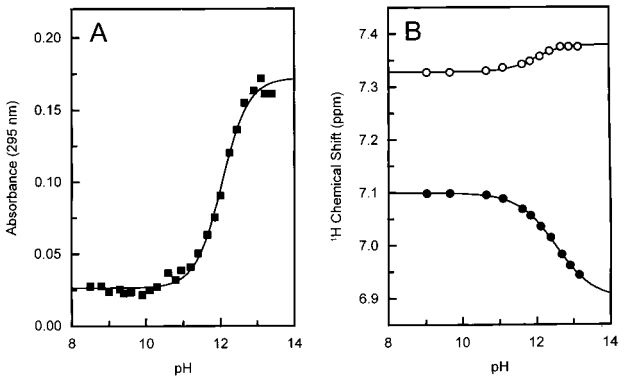

FIGURE 8: pH titrations of the phenolic hydroxyl group of tyrosine in the F50Y mutant of 4-OT monitored by UV spectroscopy (A), and ^{1}H NMR spectroscopy (B), at 23 °C. In panel A, the UV absorbances of F50Y (40 μM in subunits) at 295 nm, plotted as a function of pH ranging from 8.5 to 13.4, are fit by eq 1 using a pK_a of 12.0 ± 0.1 and a Hill coefficient (n) of 1.2 ± 0.1. In panel B, the pH dependences of the chemical shifts of the aromatic side chain δ (open circles) and ϵ (closed circles) proton resonances of Tyr-50 of the F50Y mutant (3.0 mM in subunits) are plotted over the pH range 9.0 to 13.1. The curves are computed by fitting the data to eq 1 using a pK_a of 12.0 ± 0.1 and a Hill coefficient of 1.1 ± 0.2 for the δ-protons and a pK_a of 12.5 ± 0.1 and a Hill coefficient of 0.84 ± 0.10 for the ϵ-protons.

ϵ-protons are more sensitive to pH because of their proximity to the hydroxyl group. The UV and NMR titrations together yield an average pK_a of 12.2 ± 0.3 with an average Hill coefficient of 1.0 ± 0.1 for Tyr-50.[3]

DISCUSSION

We have shown previously by the effects of appropriate arginine mutations that the nearby cationic residues Arg-11′, Arg-39″, and Arg-61′ are not responsible for the three unit decrease in the pK_a of Pro-1 in the active site of 4-OT (*14*).[2] Hence, the low pK_a of Pro-1 must result solely from a low dielectric constant (ϵ_{prot}) at the otherwise hydrophobic active site (Figure 2). Assuming this to be the case, an ϵ_{prot} value of 14.7 ± 0.8 is calculated for the active site of wild type 4-OT from the Born approximation (eq 5):

$$\Delta\Delta G^\circ = (164.9)(1/\epsilon_{prot} - 1/\epsilon_{water})/r \qquad (5)$$

using $\Delta\Delta G^\circ = 4.16$ kcal/mol, $\epsilon_{water} = 76.6$ at 30 °C, and r, the cavity radius = 2.17 Å for secondary amines (*4*, *10*, *30*, *31*).

The F50Y mutant, which is catalytically fully active (Table 1) and structurally largely intact (Figure 3, panels A−C), provides two independent measurements of the local dielectric constant, ϵ_{prot}. From the pK_a of 6.0 ± 0.1 for Pro-1, we may use eq 5 with a $\Delta\Delta G^\circ = 4.59$ kcal/mol, $\epsilon_{water} = 79.05$ at 23 °C, and $r = 2.17$ Å to obtain $\epsilon_{prot} = 13.7 \pm 0.3$, which overlaps with that of the wild-type enzyme. If indeed ϵ_{prot} is low for the F50Y mutant, then the pK_a of Tyr-50 should be significantly increased above 10.2, the pK_a of the model compound, *N*-acetyl-tyrosine amide in water (*4*). Both UV and NMR titrations yield an average p$K_a = 12.2 \pm 0.3$, which is increased by 2 units, and an average Hill coefficient of 1.0. Using eq 5 with a $\Delta\Delta G^\circ = 2.16$ kcal/mol, $\epsilon_{water} = 79.05$ at 23 °C, and $r = 3.79$ Å for the delocalized tyrosinate anion (4) yields $\epsilon_{prot} = 13.4 \pm 1.7$. This value agrees with those found by titration of Pro-1 in the F50Y mutant and also in the wild-type enzyme. Hence, the ∼3 unit decrease in the pK_a of Pro-1 and the ∼2 unit increase in the pK_a of Tyr-50 both reflect a local dielectric constant of $\epsilon_{prot} \sim 13.6 \pm 1.0$ at the active site of 4-OT.

In contrast to F50Y, the F50A mutant is both kinetically (Table 1) and structurally damaged (Figures 3−5). Most notable is the destabilization of the β-hairpin that extends from residues 50−57, and that covers the active site. This destabilization is manifested by the loss of interstrand and turn NOEs (Figure 5), by the degeneracy of the backbone ^{15}N and NH chemical shifts of Gly-48, 51, 53, and 54, and by the disappearance of these resonances at 43 °C due to rapid exchange with solvent. Thus, in the F50A mutant, replacing Phe-50 with a small residue, appears to have increased the solvent accessibility to the active site. In the X-ray structure of 4-OT, the β-hairpin of one subunit approaches the C-terminal half of the helix and the entire β2 strand of another subunit (Figure 2) (*8*, *12*). The loss of these interactions in the F50A mutant resulting from the disruption of the β-hairpin would increase solvent accessibility to these regions, which could explain the large changes in their ^{15}N and NH chemical shifts (Figure 3, panels D−F), despite their largely intact secondary structures (Figures 4 and 5). Consistent with greater solvent accessibility, the pK_a of Pro-1 has increased by ∼1 unit to values of 7.3 ± 0.1 as found by ^{15}N NMR titration (Table 2) and 7.6 ± 0.2 as found by the pH dependence of k_{cat}/K_m (Table 3). With these pK_a values, eq 5 may be used to calculate the local dielectric constant ϵ_{prot} near Pro-1 to have increased by 7 ± 3 units to 21.6 ± 2.6 in the F50A mutant.

[3] The pK_a of Tyr-50 in the F50Y mutant was also measured by monitoring the changes in tyrosine fluorescence as a function of pH. As the tyrosine is deprotonated, its fluorescence is quenched. Analysis of the fluorescence decrease with increasing pH (data not shown) yielded a pK_a of 11.1 ± 0.1 ($n = 0.9 \pm 0.1$). One explanation for this lower value is that a nearby group with this lower pK_a value, when deprotonated, quenches the fluorescence of Tyr-50. Tyrosine fluorescence is known to be sensitive to its environment (*4*).

The increase in the pK_a of Pro-1 alone, would explain at most, only a 1.5-fold loss of activity at pH 7.5. Hence, the 167-fold decrease in k_{cat} and the 11-fold increase in K_m of the F50A mutant (Table 1) likely reflect other damaging effects of increasing the local dielectric constant on catalysis and substrate binding. The decrease in k_{cat} in the F50A mutant may result from a weaker electrostatic interaction between cationic proline-1 and the anionic enolate intermediate in the rate-limiting transition state of step 2 (Figure 1) as a result of the higher dielectric constant. Similarly, the increase in K_m (11-fold) is comparable to that previously reported for the R11A mutant (9-fold), which was attributed to a loss of the interaction of Arg-11′ with the 6-carboxylate group of the substrate (Figure 1) (*13*). The structural analysis of the F50A mutant thus indicates that the increased K_m may result from weaker electrostatic interactions between the active site arginine residues and the substrate carboxylate groups in the higher dielectric environment. Alternatively, or additionally, in the wild-type enzyme, the diene portion of **2** may make an important hydrophobic interaction with the phenyl ring of Phe-50, which is lost in the F50A mutant.

A multiple sequence alignment of 4-OT and its 26 known homologues shows that Phe-50 is found in six homologues, a tyrosine occupies this position in seven homologues, and a tryptophan is present in nine homologues.[4] Thus, an amino acid with an aromatic side chain is found in all but five of the 27 known 4-OT homologues. In the remaining homologues, this position is occupied by a valine (3 cases), a methionine, or an isoleucine, amino acids having a hydrophobic side chain. These findings coupled with the fact that Phe-50 is located in the active site and is 5.8 Å from Pro-1 (*8*, *12*, *28*), suggest that a hydrophobic residue, preferably one with aromatic character, is important for the structure and mechanism of 4-OT.

The preference for an aromatic residue is reflected here in the decreased stabilities and catalytic efficiencies of the F50V and F50I mutants (Table 1).[5] While Val is less hydrophobic than Phe, as indicated by hydropathy indices, Ile is similar in hydropathy to Phe (*32*, *33*). Yet the Ile substitution is more destabilizing and catalytically damaging than the Val substitution, possibly due to the loss of the above-mentioned interaction between the diene portion of **2** and the aromatic ring of Phe-50, or to steric effects of Ile-50 which disrupt the active site and increase solvent access. Similar effects on k_{cat} are found with ketosteroid isomerase upon mutating Phe-101 to Ala and Leu (*34*). These effects have been ascribed to destabilization of the charged transition state(s) as a result of increased polarity or solvation of the active site, which would weaken hydrogen bonding of the transition state(s) by the nearby acid catalysts, Tyr-14 and Asp-99 (*35*, *36*).

ACKNOWLEDGMENT

Electrospray ionization mass spectrometry was performed by the analytical instrumentation service core supported by Center grant ES 07784. We are grateful to Patricia M. Legler for help in data collection.

[4] R. M. Czerwinski, A. Murzin, and C. P. Whitman (2000), unpublished results.

[5] Although there are 4-OT homologues with an isoleucine or a valine in place of Phe-50, these proteins have not been characterized structurally or kinetically, so it is unclear whether there are compensatory features that stabilize the protein.

REFERENCES

1. Fersht, A. R. (1999) *Structure and Mechanism in Protein Science*, pp 188−189, W. H. Freeman & Co., New York.
2. Schmidt, Jr., D. E., and Westheimer, F. H. (1971) *Biochemistry 10*, 1249−1253.
3. Highbarger, L. A., Gerlt, J. A., and Kenyon, G. L. (1996) *Biochemistry 35*, 41−46.
4. Li, Y.-K., Kuliopulos, A., Mildvan, A. S., and Talalay, P. (1993) *Biochemistry 32*, 1816−1824.
5. Thornburg, L. D., Henot, F., Bash, D. P., Hawkinson, D. C., Bartel, S. D., and Pollack, R. M. (1998) *Biochemistry 37*, 10499−10506.
6. Whitman, C. P., Aird, B. A., Gillespie, W. R., and Stolowich, N. J. (1991) *J. Am. Chem. Soc. 113*, 3154−3162.
7. Lian, H., and Whitman, C. P. (1993) *J. Am. Chem. Soc. 115*, 7978−7984.
8. Subramanya, H. S., Roper, D. I., Dauter, Z., Dodson, E. J., Davies, G. J., Wilson, K. S., and Wigley, D. B. (1996) *Biochemistry 35*, 792−802.
9. Stivers, J. T., Abeygunawardana, C., Mildvan, A. S., Hajipour. G., Whitman, C. P., and Chen, L. H. (1996) *Biochemistry 35*, 803−813.
10. Stivers, J. T., Abeygunawardana, C., Mildvan, A. S., Hajipour. G., and Whitman, C. P. (1996) *Biochemistry 35*, 814−823.
11. Czerwinski, R. M., Johnson Jr., W. H., Whitman, C. P., Harris, T. K., Abeygunawardana, C., and Mildvan, A. S. (1997) *Biochemistry, 36*, 14551−14560.
12. Taylor, A. B., Czerwinski, R. M., Johnson, Jr., W. H., Whitman, C. P., and Hackert, M. L. (1998) *Biochemistry 37*, 14692−14700.
13. Harris, T. K., Czerwinski, R. M., Johnson, Jr., W. H., Legler, P. M., Abeygunawardana, C., Massiah, M. A., Stivers, J. T., Whitman, C. P., and Mildvan, A. S. (1999) *Biochemistry 38*, 12343−12357.
14. Czerwinski, R. M., Harris, T. K., Johnson, Jr., W. H., Legler, P. M., Stivers, J. T., Mildvan, A. S., and Whitman, C. P. (1999) *Biochemistry 38*, 12358−12366.
15. Whitman, C. P., Czerwinski, R. M., Harris, T. K., and Mildvan, A. S. (2000) *Biochemistry 39*, 1549, Abs No. 34.
16. Sambrook, J., Fritsch, E. F., & Maniatis, T. (1989) *Molecular Cloning: A Laboratory Manual*, Cold Spring Harbor Laboratory, Cold Spring Harbor, NY.
17. Chen, L. H., Kenyon, G. L., Curtin, F., Harayama, S., Bembenek, M. E., Hajipour, G., and Whitman, C. P. (1992) *J. Biol. Chem. 267*, 17716−17721.
18. Waddell, W. J. (1956) *J. Lab. Clin. Med. 48*, 311−314.
19. Ho, S. N., Hunt, H. D., Horton, R. M., Pullen, J. K., and Pease, L. R. (1989) *Gene 77*, 51−59.
20. Marion, D., Driscoll, P. C., Kay, L. E., Wingfield, P. T., Bax, A., Gronenborn, A. M., and Clore, G. M. (1989) *Biochemistry 28*, 6150−6156.
21. Levy, G. C., and Lichter, R. L. (1979) in *Nitrogen-15 NMR Spectroscopy*, John Wiley & Sons, Inc., New York.
22. Weber, D. J., Abeygunawardana, C., Bessman, M. J., and Mildvan, A. S. (1993) *Biochemistry 32*, 13081−13088.
23. Johnson, B. A., and Blevins, R. A. (1994) *J. Biomol. NMR 4*, 603−614.
24. Delaglio, F., Grzesiek, S., Vuister, G., Zhu, G., Pfeifer, J., and Bax, A. (1995) *J. Biomol. NMR 6*, 277−293.
25. Mori, S., Abeygunawardana, C., Johnson, M. O., and van Zijl, P. C. M. (1995) *J. Magn. Reson. 103B*, 203-216.
26. Zhao, Q., Abeygunawardana, C., and Mildvan, A. S. (1997) *Biochemistry 36*, 3458−3472.
27. Kay, L. E., Keifer, P., and Saarinen, T. (1992) *J. Am. Chem. Soc. 114*, 10663−10665.
28. Stivers, J. T., Abeygunawardana, C., Whitman, C. P., and Mildvan, A. S. (1996) *Protein Sci. 5*, 729−741.

29. Wuthrich, K. (1986) *NMR of Proteins and Nucleic Acids*, p 17, John Wiley & Sons, Inc., New York.
30. Rashin, V., and Honig, B. (1985) *J. Phys. Chem. 89*, 5588−5593.
31. Friedman, H. L., and Krishan, C. V. (1973) *Water. A Comphrensive Treatise* (Franks, F., Ed.) Vol. 3, pp 1−118, Plenum Press, New York.
32. Engelman, D. M., Steitz, T. A., and Goldman, A. (1986) *Annu. Rev. Biophys. Biophys. Chem*. *15*, 321−353.
33. Fauchere, J. L., and Pliska, V. (1983) *Eur. J. Med. Chem. 18*, 369−375.
34. Brothers, P. N., Blotny, G., Qi, L., and Pollack, R. M. (1995) *Biochemistry 34*, 15453−15458.
35. Zhao, Q., Abeygunawardana, C., Gittis, A., and Mildvan, A. S. (1997) *Biochemistry 36*, 14616−14626.
36. Qi, L., and Pollack, R. M. (1998) *Biochemistry 37*, 6760−6766.

BI0024714